Biophysical Chemistry 171 (2013) 1–8

Contents lists available at SciVerse ScienceDirect

Biophysical Chemistry

journal homepage: http://www.elsevier.com/locate/biophyschem

Isothermal quadruplex priming amplification for DNA-based diagnostics

Adam Taylor [a], Anupama Joseph [a], Robert Okyere [a], Shota Gogichaishvili [a,b], Karin Musier-Forsyth [a], Besik Kankia [a,c,*]

[a] Department of Chemistry and Biochemistry, Center for RNA Biology, The Ohio State University, Columbus, OH 43210, USA
[b] Andronikashvili Institute of Physics, Tbilisi 0177, Republic of Georgia
[c] Institute of Biophysics, Ilia State University, Tbilisi 0162, Republic of Georgia

HIGHLIGHTS

- Driving force of QPA comes from the thermal stabilities of primer/template and product complexes.
- Primers missing one and two guanines are able to self-dissociate from the template upon elongation.
- QPA is not observed when the primer lacks three nucleotides.
- QPA reaches its maximum rate at temperatures slightly higher than the T_m of primer/template complex.
- *Taq* is able to incorporate T opposite template 2AP, while no activity was observed for 6MI.

GRAPHICAL ABSTRACT

Scheme showing linear QPA, which isothermally amplifies the DNA signal and allows real-time monitoring through incorporated fluorescence nucleotides.

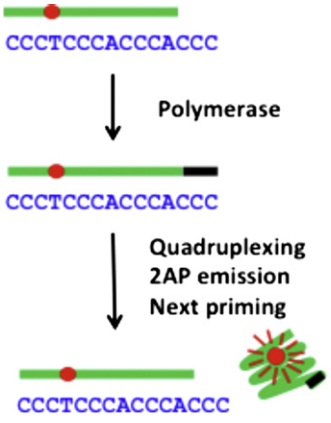

ARTICLE INFO

Article history:
Received 11 October 2012
Received in revised form 5 November 2012
Accepted 6 November 2012
Available online 14 November 2012

Keywords:
DNA quadruplex
2-aminopurin
6-methylisoxanthopterin
Fluorescence
Thermodynamics
DNA amplification

ABSTRACT

We previously developed a method, known as quadruplex priming amplification (QPA), which permits isothermal amplification of DNA. The assay is based on a DNA quadruplex formed by the GGGTGGGT GGGTGGG (G3T) sequence. G3T has three unique properties that are fundamental for QPA; (i) G3T forms a quadruplex with significantly more favorable thermodynamics than the corresponding DNA duplexes; (ii) removal of guanines at the 3′-end inhibits quadruplex formation; and (iii) incorporated fluorescent nucleotides, such as 2-aminopurine (2AP) or 6-methylisoxanthopterin (6MI), which are quenched by neighboring nucleotides, regain maximum emission upon quadruplex formation. New model studies carried out here with primers missing one, two and three guanines reveal that the driving force for QPA comes from the difference in thermal stability between the primer/template and the product complexes. Primers missing one and two guanines are able to self-dissociate from the template upon elongation, whereas QPA is not observed when the primer lacks three 3′-nucleotides. QPA reaches its maximum rate at temperatures slightly higher than the T_m of the primer/template complex and is more

* Corresponding author at: Department of Chemistry and Biochemistry, Center for RNA Biology, The Ohio State University, Columbus, OH 43210, USA. Tel.: +1 614 688 8799; fax: +1 614 688 5402.
E-mail address: kankia.1@osu.edu (B. Kankia).

0301-4622/$ – see front matter
http://dx.doi.org/10.1016/j.bpc.2012.11.001

efficient in the presence of only dGTP. QPA-based assays also revealed that *Taq* is able to incorporate thymidines opposite template 2AP, while no significant incorporation was observed opposite template 6MI.

1. Introduction

Real-time polymerase chain reaction (RT-PCR), which allows for amplification and quantification of DNA from specimens containing even low concentrations of DNA, is the method of choice for detection of pathogenic microorganisms and genetic diseases [1,2]. However, temperature cycling, limited yield of product DNA, low specificity, the need for specialized instruments and expensive detection probes restrict wide usage of RT-PCR in molecular diagnostics. Recently, we have described quadruplex priming amplification (QPA), a novel assay for DNA amplification and quantification [3]. Specifically, we have found that the free energy of DNA quadruplexes can be used to drive unfavorable (endergonic) reactions (e.g., DNA amplification requiring temperature cycling) at constant temperature. A key aspect of QPA is that some G-rich sequences are capable of forming quadruplexes with significantly more favorable thermodynamics than the corresponding DNA duplexes. The primer, which is based on such sequences, is designed to spontaneously dissociate from the primer binding sites (PBS) and fold into a monomolecular quadruplex upon polymerase elongation. In addition, primers containing fluorescent nucleotides in the loop positions demonstrated almost 100-fold increase in fluorescence upon quadruplex formation, which permits simple and effective quantification without extra probe molecules [3].

One of the major disadvantages of polymerase-based diagnostics is its low specificity [2]. Due to the nonspecific nature of DNA polymerases, any 5′ overhang can serve as a substrate and initiate DNA replication. The complex nature of the RT-PCR mixture (forward and reverse primers, probe, all four dNTPs and polymerase) and thermocycling facilitate non-specific product formation caused by primer-dimerization and mis-priming. In addition, non-specific probe hybridization also creates false positive signals. QPA has the potential to increase the specificity of nucleic acid diagnostics. First, since the signal amplification scheme described in Fig. 1 requires only dGTP, one can remove dATP, dCTP and dTTP from the reaction mixture. This will inhibit any non-specific DNA production. Second, non-specific binding of the QPA primer is not sufficient to produce a false signal; to create a false signal the 3′-end of the QPA primer has to bind non-specifically near two or more cytidines. Thus, it is unlikely that non-specific priming can create a false positive in QPA. Third, QPA requires only one primer, which removes the possibility of primer-dimerization. Fourth, amplification proceeds isothermally, which prevents mis-priming due to temperature-induced DNA structural changes. As such, QPA has the potential to amplify nucleic acids with high specificity.

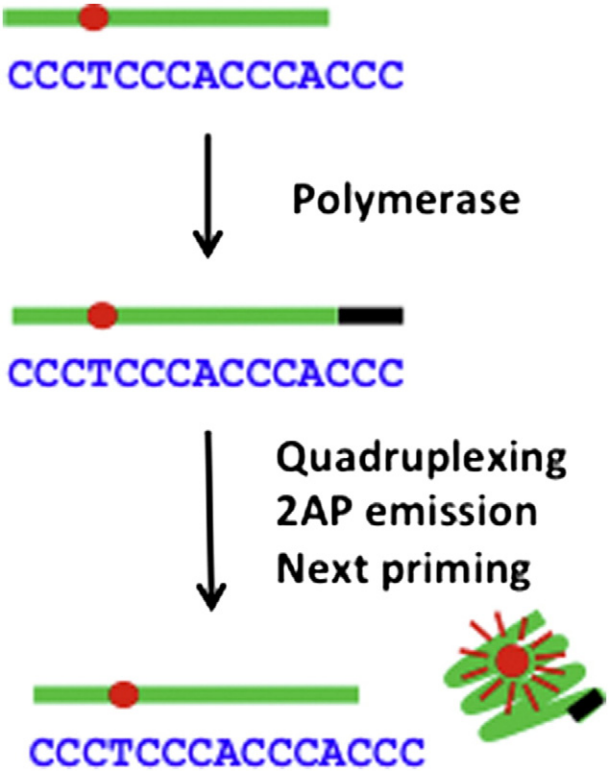

Fig. 1. Scheme showing linear QPA, which isothermally amplifies the DNA signal and allows real-time monitoring through incorporated fluorescence nucleotides.

In the present work a model system was used to investigate the role of reaction components and conditions (temperature, dNTP concentrations, K^+ concentration, primer length, primer/template stability) in linear QPA. We also studied QPA-related activities of *Taq* polymerase including dNTP incorporation opposite template fluorescent nucleotides; dGTP incorporation opposite natural nucleotides; and extension speed in the absence of certain dNTPs. The data reported here creates a framework for the further development and applications of QPA in nucleic acid-based diagnostics.

2. Experimental procedures

2.1. Enzymes and DNA substrates

Taq polymerase was purchased from New England BioLabs. DNA oligonucleotides were obtained from Integrated DNA Technologies and Fidelity Systems. The concentration of DNA oligonucleotides was determined by measuring UV absorption at 260 nm as described earlier [4]. All measurements were performed in a buffer solution consisting of 10 mM Tris–HCl at pH 8.7; ionic strength was adjusted by addition of appropriate salt.

2.2. Fluorescence, CD and UV spectroscopy

UV absorption readings during temperature unfolding experiments were taken at either 240 nm, 260 nm, or 295 nm as a function of temperature using a Varian UV–visible spectrophotometer (Cary100 Bio). Fluorescence measurements of 2AP (ex 310 nm, em 370 nm) and 6MI (ex 340 nm, em 430 nm) were performed using a Varian spectrophotometer (Cary Eclipse). CD spectra were obtained with a Jasco-815 spectropolarimeter. All optical devices were equipped with thermoelectrically controlled cell holders. In a typical experiment, oligonucleotide samples were mixed and diluted into the desired buffers in optical cuvettes. The solutions were incubated at 95 °C for a few min in the cell holder prior to ramping to the desired starting temperature. In the case of DNA duplexes, to ensure that the quadruplex-forming sequence formed a double helix with its complementary strand, the sequences were annealed in CsCl and $MgCl_2$ containing buffers and KCl was added later. After annealing, the temperature was then ramped to the desired starting temperature, KCl was added and the melting experiments were performed at a heating rate of 0.5 or 1 °C/min. The melting curves allowed an estimate of melting temperature, T_m, the midpoint temperature of the unfolding process. Van't Hoff enthalpies, ΔH_{vH}, were also calculated using the following equations: $\Delta H_{vH} = 4RT_m^2\ \delta\alpha/\delta T$ in the

case of monomolecular quadruplexes and $\Delta H_{vH} = 6\ RT_m^2\ \delta\alpha/\delta T$ in the case of bimolecular DNA duplexes, in which R is the gas constant and $\delta\alpha/\delta T$ is the slope of the normalized optical absorbance or fluorescence versus temperature curve at the T_m [5].

2.3. Polymerase activity assay

The enzymatic activity of *Taq* polymerase was monitored using a real-time quadruplex formation assay (QFA), which is based on similar assays employed earlier for nucleic acid strand-exchange [6] and cleavage [7] reactions. The assay takes advantage of the unique thermodynamic and fluorescence properties of the GGGTGGGTGGGTGGG (G3T) sequence. As mentioned above, this sequence is able to form a monomolecular DNA quadruplex consisting of three G-quartets [8,9]. The G-quartets are connected with chain-reversal single-nucleotide loops, which are completely open to solvent and represent convenient positions for incorporation of fluorescent nucleotides [8,9]. The quadruplex structure is unusually stable. For instance, in the presence of 50 mM KCl (quadruplex forming cation), G3T melts above 100 °C, while in the presence of same amount of CsCl, its corresponding duplex unfolds around 60 °C [9]. In addition, quadruplex formation is accompanied by strong emission of fluorescence when 2AP or other fluorescent nucleotides are incorporated at loop positions. The truncated version of G3T is not able to fold the quadruplex and perfectly hybridizes with the template, which represents a complementary sequence to G3T (Fig. 1). A polymerase attaches missing guanines and, as a result, G3T spontaneously dissociates from its template, folds into the quadruplex and emits light. All template and primer sequences are collected in Table 1. QPA reactions were carried out in a reaction mixture containing 200 μM of each dNTP or 800 μM of dGTP, buffer (2 mM $MgCl_2$, 25 mM CsCl, 25 mM KCl, 10 mM Tris–HCl, pH 8.7) and 0.05 unit/μL *Taq* polymerase. The reactions were carried out directly in the quartz cuvettes. In a typical experiment, 10× buffer, dNTP and *Taq* were added. The solution was vortexed for 2–3 seconds and immediately inserted into a cell holder of the fluorometer equilibrated at reaction temperature followed by real-time fluorescence monitoring.

2.4. Incorporation of guanine opposite template adenine and thymidine

The assay was performed essentially as described in the previous section. The templates with one or two mismatches (underlined), designed for a 13-nt primer with incorporated 6MI (**G**), are shown below:

Primer: 5′GGG**G**GGGCGGGCG
Templates: 3′CCCCCCCGCCCGCAC
3′CCCCCCCGCCCGCAA

Table 1
Melting temperatures (T_m) and optimal temperature for QPA (T_{QPA}) of the primer/template complexes[a].

Primer/template sequence	T_m (°C)		$\Delta T_{m,\ Sub\text{-}Prod}$ (°C)	T_{QPA} (°C)
	Cs^+	K^+		
5′GGG**A**GGGCGGGCGGG (Product) 3′CCCTCCCGCCCGCCC	75.0 (68.4)	69.0	-	-
5′GGG**A**GGGCGGGC (Sub1) 3′CCCTCCCGCCCGCCC	67.0 (58.0)	68.0	−1.0	nd
5′GGG**A**GGGCGGGCG (Sub2) 3′CCCTCCCGCCCGCCC	70.5 (62.5)	71.0	2.0	65.0
5′GGG**A**GGGCGGGCGG (Sub3) 3′CCCTCCCGCCCGCCC	73.0 (65.7)	73.5	4.5	67.0

Values in parentheses correspond to T_m of the duplexes at 100 nM strand concentration estimated from nearest-neighbor analysis. Duplexes are measured in either in K^+ buffer (25 mM KCl, 25 mM CsCl, 2 mM $MgCl_2$, 10 mM Tris–HCl, pH 8.7) or in Cs^+ buffer (50 mM CsCl, 2 mM $MgCl_2$, 10 mM Tris–HCl, pH 8.7). $\Delta T_{m,\ Sub\text{-}Prod}$ corresponds to the T_m difference between primer/template and full-length duplexes in K^+ buffer. T_{QPA} corresponds to the optimal experimental temperature for QPA.

3′CCCCCCCGCCCGCCA
3′CCCCCCCGCCCGCTC
3′CCCCCCCGCCCGCTT
3′CCCCCCCGCCCGCCT
3′CCCCCCCGCCCGCGC
3′CCCCCCCGCCCGCGG
3′CCCCCCCGCCCGCCG

The assay was conducted in the presence of only dGTPs, and the fluorescence signal of 6MI (ex 340 nm, em 430 nm) was monitored.

2.5. Incorporation of nucleotides opposite template 2AP and 6MI

In this assay, the following primer and templates were used (**A** = 2AP, **G** = 6MI):

Primer: 5′GCGCGGG**A**GGGCGGG
Templates: 3′CGCGCCCTCCCGCCC**A**CCC
3′CGCGCCCTCCCGCCC**G**CCC
Controls: 3′CGCGCCCTCCCGCCCACCC
3′CGCGCCCTCCCGCCCGCCC

The QFA assay was performed as described in the previous sections with two changes. First, the amplification was conducted under temperature cycling conditions (65 °C–0.5 min, 77 °C–1 min, 90 °C–0.2 min) in order to facilitate both primer binding and product dissociation processes. Second, amplification was performed in the presence of different mixtures of dNTPs: only dGTP, dGTP + dATP, dGTP + dTTP and dGTP + dCTP.

3. Results and discussion

3.1. Optimal temperature for isothermal QPA

Fig. 1 shows the model QPA reaction scheme used in these studies. To determine the optimal reaction temperature for QPA, we used three primers based on a quadruplex-forming sequence with 2AP and cytosines in loop positions (see Table 1). To ensure that the nucleotide exchange in the loop position did not hinder the quadruplex forming ability of the full-length sequence, CD studies were performed. No significant effects due to the modifications were observed (data not shown). The primers were missing three (Sub1), two (Sub2) and one (Sub3) of the 3′-end guanines (Table 1). As discussed above, the isothermal nature of QPA is based on the fact that upon polymerase elongation, the primer spontaneously dissociates from the PBS and forms a quadruplex. Thus, the primer/PBS complex (substrate) has to be more stable than the same complex after elongation (product). To compare thermal stabilities of the substrates and products, UV melting experiments were performed for all complexes shown in Table 1. Fig. 2 shows typical unfolding experiments for all complexes in the presence (panel A) and absence (panel B) of K^+ ions. In the presence of K^+ ions, the full-length duplex (panel A, black) unfolds at 69.0 °C, and in the absence of K^+ ions, the duplex is significantly more stable and unfolds at 75.0 °C (panel B, black) as predicted from nearest-neighbor analysis of equilibrium unfolding [10]. Fig. 2 also demonstrates unfolding of primer/template complexes in the presence (Panel A) and absence (Panel B) of K^+ ions. Since truncated versions are not able to form a quadruplex [3,9], the melting profiles are similar in the presence and absence of K^+ ions (Table 1). As expected, in the presence of Cs^+ ions, the full-length duplex (Product) is more stable than the shorter duplexes; removal of each G•C base-pair is accompanied by a decrease of ~2–3 °C in thermal stability. In the presence of K^+ ions, the shortest duplex (Sub1) and the product duplex melt at the same temperature, ~68 °C, while Sub2 and Sub3 are more stable with melting temperatures of 71.0 °C and 73.5 °C, respectively. Thus, in the presence of K^+ ions, the 13-bp and 14-bp duplexes are more stable than the 15-bp

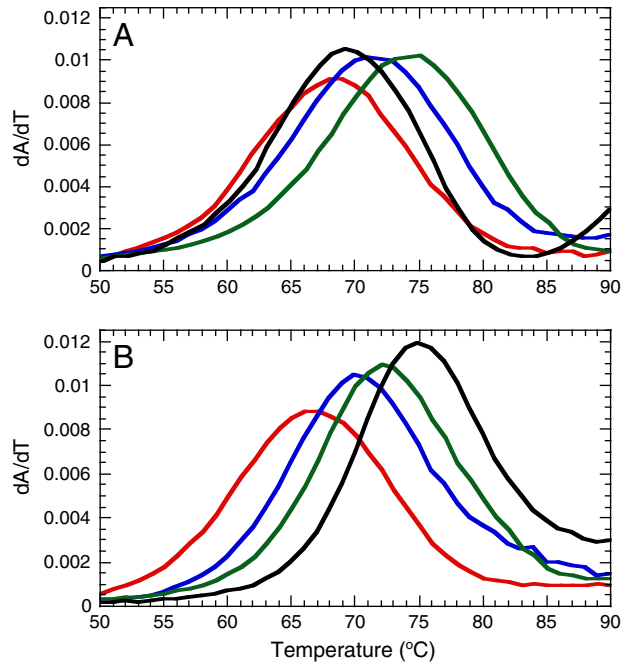

Fig. 2. UV melting curves of Sub1 (red), Sub2 (blue) and Sub3 (green) and their blunt end variant (product) (black) in the presence of K^+ ions (25 mM KCl, 25 mM CsCl, and 2 mM $MgCl_2$) (panel A) and in the absence of K^+ ions (50 mM CsCl and 2 mM $MgCl_2$) (panel B).

full-length duplex. This unusual result is due to the non-equilibrium nature of the transition in the presence of quadruplex-forming K^+ ions; unfolding of the duplex is accompanied by quadruplex formation of the released strands, which inhibits the reverse reaction (duplex refolding) and, as a result, shifts it to lower temperatures. Thus, in the case of Sub2 and Sub3, the primer/template complex is more stable than its elongated version, the full-length duplex, which facilitates product dissociation.

Fig. 3 demonstrates the dependence of QPA rate on temperature. In the case of Sub1, we do not observe strong activity over the entire temperature range. The temperature- dependence experiments using Sub2 demonstrate significant activity between 60 °C and 70 °C with a maximum at ~65 °C. The rate of QPA steadily increases from 60 °C to 65 °C and decreases between 65 °C and 70 °C. In the case of Sub3, missing only one guanine, QPA activity is observed over a wider temperature range, from 60 to 75 °C. At the maximum, 67–68 °C, the rate reaches 8 nM/min, which is ~30% higher than the rate for Sub2. Both profiles resemble the melting peak of a DNA duplex. Interestingly, the

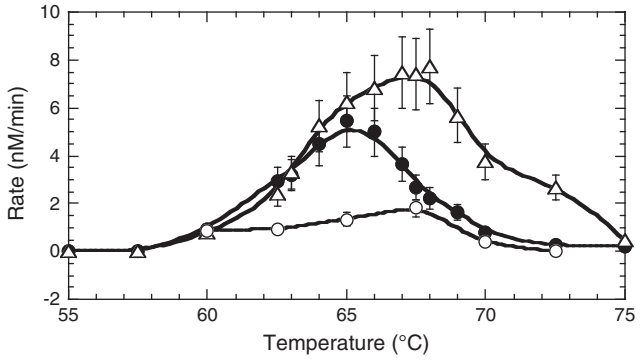

Fig. 3. QPA rate dependence on temperature using Sub1 (open circles), Sub 2 (closed circles) and Sub3 (triangles) in 25 mM KCl, 25 mM CsCl, 2 mM $MgCl_2$, 10 mM Tris–HCl, pH 8.7 at 20 °C.

maximum value of QPA rate for Sub3, which has an extra G•C base pair, is 2–3 °C higher than the same parameter for Sub2. The difference is equal to a contribution of an extra G•C base pair to thermal stability [10]. Thus, the temperature dependence of QPA rates closely correlates with the melting behavior of the complexes, which agrees with the idea that the nature of QPA is determined by thermal stabilities of the primer/template complexes before and after elongation [3]. Careful inspection of Table 1 further supports the idea. Sub1, which does not reveal strong QPA activity, is slightly less stable than the product duplex. Thus, the elongation process has a slight stabilizing effect on the complex, and the product cannot self-dissociate effectively within the entire temperature range shown in Fig. 3. Thus, Sub1 does not allow efficient priming and product self-dissociation at the same temperature. At lower temperatures, primers bind to templates, but they are not able to dissociate. At higher temperatures, for which Sub1 shows slightly better activity, primers are not able to bind the PBS efficiently. Sub2 and Sub3 demonstrate good QPA activity because both of them are destabilized upon elongation by 2 °C and 4.5 °C, respectively (Table 1). In addition, Sub3, which has the greatest destabilizing effect on QPA rate, reaches the highest level and is active over wider temperature range (Fig. 3). Between 60 °C and 65 °C, both Sub2 and Sub3 demonstrate similar increases in QPA rate (Fig. 3). At 65 °C, Sub2 reaches its rate maximum, and a further increase in temperature is accompanied by a decline in QPA rate. In the case of Sub3, the peak is around 67–68 °C (Fig. 3).

Further steps were taken to determine the rate-limiting step of QPA. In a typical reaction, the catalytic cycle of DNA polymerase consists of the following steps: (i) primer binding to PBS; (ii) polymerase binding to primer/template complex; (iii) binding of dNTP; (iv) sampling of correct dNTP; (v) structural change of the complex; (vi) nucleotide incorporation; (vii) pyrophosphate release; and (viii) polymerase dissociation. It is known that for nonprocessive DNA synthesis, enzyme dissociation is the rate-limiting step, since all other steps are significantly faster [11–13]. In QPA, besides the steps listed above, there is an additional step at the end of the reaction: product dissociation. This step can occur spontaneously or could be facilitated by strand-displacement by incoming primers. It is clear that enzyme dissociation cannot be responsible for the rate behavior shown in Fig. 3, since polymerase binding/dissociation properties show little temperature dependence under the experimental conditions employed here [14,15]. Thus, it is reasonable to assume that product dissociation/displacement is responsible for the observed behavior and represents the rate-limiting step in QPA. Sub2 and Sub3 differ from each other only by primer length, since the final product for both of them, the full-length duplex, is the same. Thus, at the temperatures for which we could have similarly efficient priming for both of the primers, we would expect the same rates. Indeed, between 60 °C and 65 °C, both systems demonstrate the same QPA rates (Fig. 3). Above 65 °C, corresponding to the T_m for Sub2, the rates deviate: Sub3 continues a strong increase, while Sub2 reaches its maximum at 65 °C and starts declining (Fig. 3, filled circles). For Sub3, a similar decline starts after 68 °C; however, its maximum rate is around 30% faster than that of Sub2, which can be explained by faster dissociation or strand-displacement reactions at higher temperatures. In other words, at 68 °C, due to the extra G•C base pair, Sub3 primes more efficiently than Sub2, while the product, which is the same for both substrates, dissociates faster at this elevated temperature. The temperature difference between maximum rates is ~3 °C, which is the same as the difference in T_m values for Sub2 and Sub3. This difference is also indicates that the rate-limiting step of QPA being associated with the folding/unfolding properties of the complexes and not polymerase dissociation.

To conduct QPA at optimal temperatures for *Taq* activity (~75 °C), we designed a primer with six extra G•C base pairs at the 5′-end, 5-GCGC GCGGG**A**GGGTGGGTG. Since the primer/template complex is highly stable, $T_m = 73$ °C, it revealed almost no difference between melting temperatures of substrate and product duplexes, $\Delta T_{m,\ \text{Sub-Prod}} \approx 0$.

However, this primer demonstrated strong QPA activity between 70 °C and 80 °C with a maximum rate of 9 nM/min at 75 °C (data not shown). In agreement with the data collected in Table 1, 5′GCGCGC GGG**A**GGGTGGGTG primer also reaches maximum QPA rate at temperatures slightly higher than the T_m of the primer/template complex. Taken together, the present study demonstrates that QPA is able to carry out robust isothermal amplification over essentially the entire temperature range suitable for *Taq* activity (between 60 °C and 80 °C).

3.2. Dependence of QPA rate on potassium concentration

K^+ ions play a key role and can have both positive and negative effects on QPA. In order to have exponential growth, DNA polymerase must invade and replicate the quadruplex at the 5′-end of the template [3], which could be impeded by high stability of the quadruplex in the presence of high concentrations of K^+ ions. At the same time, increasing K^+ concentration accelerates QPA by facilitating dissociation of primers. Here, we studied the role of K^+ concentration in linear QPA. In these experiments, the total amount of monovalent cations (K^+ and Cs^+) is kept constant, while the amount of K^+ is varied. Fig. 4 demonstrates the dependence of QPA rate on K^+ concentration. For both the active 13-nt (triangles) and 14-nt (circles) primers similar behavior was observed. Initially, the rate increases and reaches its maximum value (~4 nM/min for 13-nt primer and ~6 nM/min for 14-nt primer) around 25 mM of K^+. Further increase in K^+ concentration is accompanied by a decrease in the rate. The decrease is somewhat stronger for the 14-nt primer; however, at 50 mM K^+, both primers have the same rate, ~3.5 nM/min. The decrease in QPA rate, which accompanies the increase of K^+ concentration between 25 mM and 50 mM, appears somewhat at odds with the QPA principle, which assumes a stronger driving force for higher amounts of K^+ ions. However, as reported earlier, truncated versions of the G3T sequence (e.g. our primers) can fold some quadruplexes at higher K^+ concentrations, especially the sequence missing only one guanine [9]. Thus, the decrease in QPA rate at higher than 30 mM K^+ ions can be attributed to the secondary structure of the primers, which impede the priming process of QPA. Another albeit less probable explanation could be related to the concentration ratio of K^+ and Cs^+ ions, $[K^+]/[Cs^+]$, which varies upon increase of K^+ concentration. Note, we keep the total amount of monovalent cations (K^+ and Cs^+) constant and only change the $[K^+]/[Cs^+]$ ratio. In our experiments, we use Cs^+ ions because they do not support any quadruplex formation [16], while other cations (such as Na^+) can form quadruplexes of different stability and topology [17,18]. Thus, Cs^+ ions allow us to keep ionic strength constant without affecting or creating a new quadruplex species. However, the Cs^+ ion is significantly larger than the K^+ ion (1.7 Å vs 1.3 Å), which can affect complex formation between DNA and *Taq*.

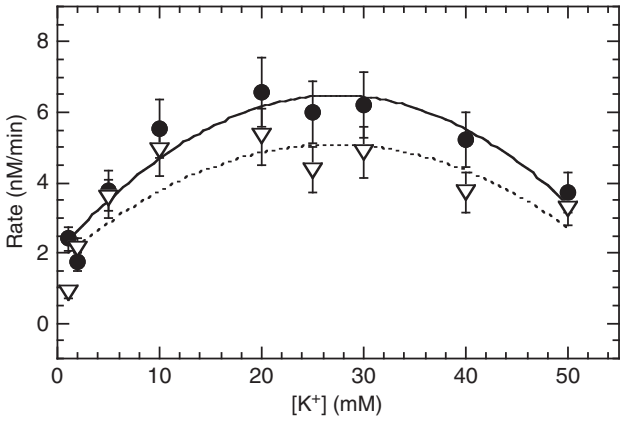

Fig. 4. QPA rate dependence on K^+ concentration using Sub2 (triangles) and Sub 3 (circles). Measurements are carried out at 65 °C in 50 mM total monovalent cations ($Cs^+ + K^+$), 2 mM $MgCl_2$, 10 mM Tris–HCl, pH 8.7 at 20 °C.

Therefore, we speculate that at low values of $[K^+]/[Cs^+]$, *Taq* dissociates at an accelerated rate, while at higher $[K^+]/[Cs^+]$ values, the dissociation rate slows down.

3.3. QPA in the presence of dGTP

As shown in Fig. 1, QPA signal production requires only dGTP. Thus, QPA can be performed in the absence of all other dNTPs (dATP, dCTP and dTTP). This has two obvious advantages: (i) the amplification buffer contains fewer components, which simplifies the amplification process; and (ii) the amplification process becomes highly specific, since DNA polymerase is not able to produce non-specific DNA.

To determine whether QPA efficiency is sensitive to dNTP composition, we performed a G-extension assay in the absence (dGTP-QPA) and presence (dNTP-QPA) of dATP, dCTP and dTTP. Fig. 5 shows QPA rate, performed on Sub3, as a function of dGTP concentration for dGTP-QPA (filled triangles) and dNTP-QPA (open circles). This study revealed that dGTP-QPA is more efficient than dNTP-QPA over the entire concentration range; more specifically, dGTP-QPA demonstrates significant (~30%) activity at very low concentrations (0.5–1 μM) of dGTP. dNTP-QPA does not demonstrate any measurable activity at these concentrations. Increasing the concentration results in an increase in QPA rate for both assays; however, in the case of dGTP-QPA, the increase is more robust, and almost full activity is observed around 20 μM of dGTP, while for dNTP-QPA, similar activity is seen around 50 μM of dGTP (Fig. 5). The efficiency of dGTP-QPA reaches its maximum at 800 μM of dGTP, which is followed by a rapid decrease in activity. In the case of dNTP-QPA, maximum efficiency is reached much earlier, at 200 μM.

All assays performed here are under steady-state conditions, and the catalytic cycle of *Taq* polymerase consists of the steps listed earlier. Thus, the only difference between the dNTP-QPA and dGTP-QPA assays is that the later is missing the sampling step. Since the QPA assays, described in Fig. 5, incorporate only one dGTP at optimal dNTP concentrations (20–800 μM dGTP for dGTP-QPA and 50–200 μM dNTP for dNTP-QPA), product dissociation is the rate-limiting step. As a result, both assays show similar rates under these conditions. However, at lower concentrations, dNTP binding slows down, and it is reasonable to conclude that, *Taq* dissociates from the primer/template complex before finding dGMP. In addition, with dGTP-QPA, *Taq* is able to demonstrate measurable activity even at 0.5 μM dGTP because it omits the selection process.

Overall, dGTP-QPA has the following advantages over dNTP-QPA: (i) the amplification mix contains less compounds; (ii) non-specific DNA production is completely inhibited; and (iii) amplification can be performed in significantly wider ranges of dGTP concentration, from 5 to 800 μM. Thus, signal production in dGTP-QPA is essentially not limited by the concentration of dGTP.

3.4. Guanine misincorporation

The efficiency of QPA in the presence of dGTP alone has tremendous potential to increase the specificity of nucleic acid diagnostics. Removal of all other dNTPs from the reaction mixture should inhibit non-specific DNA production, which is a major problem with polymerase-based diagnostics [19,20]. In addition, QPA specificity is further increased by the fact that non-specific priming alone cannot produce a false signal, since chances that a primer will randomly bind at two cytosines (required for a false signal) are only ~6%. At all other sequences, the primer would add non-G nucleotides, which would inhibit quadruplex formation and be transparent to our detection mechanism [9]. The latter relies on the high fidelity of DNA polymerases [21–23]. To test whether *Taq* indeed fails to misincorporate dGTPs opposite non-C template nucleotides additional studies have been performed using a QFA-based assay. The assay is similar to the dGTP-QPA assay, shown in Fig. 1, however in the

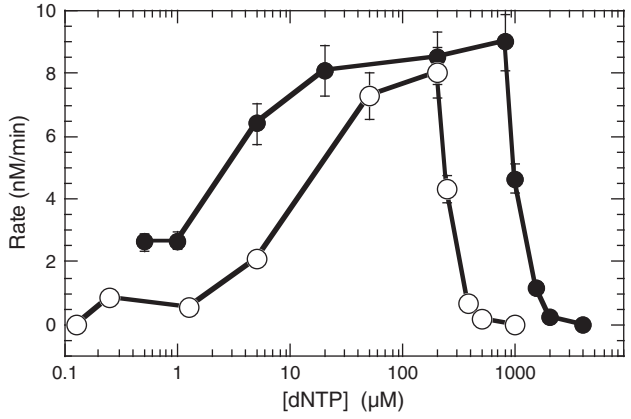

Fig. 5. QPA rates as a function of dNTP and dGTP concentration in 25 mM KCl, 25 mM CsCl, 2 mM $MgCl_2$, 10 mM Tris–HCl, pH 8.7 at 20 °C. Open circles correspond to concentration of each dNTP and closed circles correspond to concentration of dGTP alone.

14th and 15th positions of the target sequence, A, T and G have been incorporated. For each nucleotide, three types of constructs have been studied wherein (i) one incorrect nucleotide is present in the 14th position followed by a correct terminal C; (ii) both terminal nucleotides are incorrect; and (iii) a single terminal nucleotide is incorrect. The kinetic assay shown in Fig. 6A demonstrates that *Taq* is not able to efficiently misincorporate dGTP opposite to any non-C template nucleotide. Templates with A and G in the 14th position (single-nucleotide exchanges) and AA and GG at the 5′-end demonstrate no measurable elongation or misincorporation of dGTPs in these positions. However, single-nucleotide substitution in the terminal position reveals around 5% activity of the positive control (Fig. 6). In the case of two T substitutions, all three constructs (TC, CT and TT in positions 14/15) show ~10% activity. Thus, *Taq* is not able to misincorporate dGTPs with significant efficiency. Only in the case of template thymidines does QPA achieve around 10% activity relative to a positive control (template C).

3.5. Nucleotide incorporate opposite template 2AP and 6MI

In exponential QPA, DNA polymerase must be able to replicate the quadruplex sequence to create primer-binding sites in newly generated amplicons [3]. Since fluorescent nucleotides (e.g. 2AP and 6MI) are part of the quadruplexes, DNA polymerases must also be able to use these nucleotides as a template and incorporate nucleotides opposite to them. Since 2AP and 6MI show almost perfect base pairing with thymidine and cytosine, respectively [24–28], we expected the most efficient incorporation of these nucleotides.

In the present work, the ability of *Taq* polymerase to discriminate between natural and fluorescent nucleotides has been investigated using two assays. Initially, the isothermal assay described in Fig. 6 was employed, testing dGTP incorporation opposite template fluorescent nucleotides. The data (not shown) revealed no measurable QPA

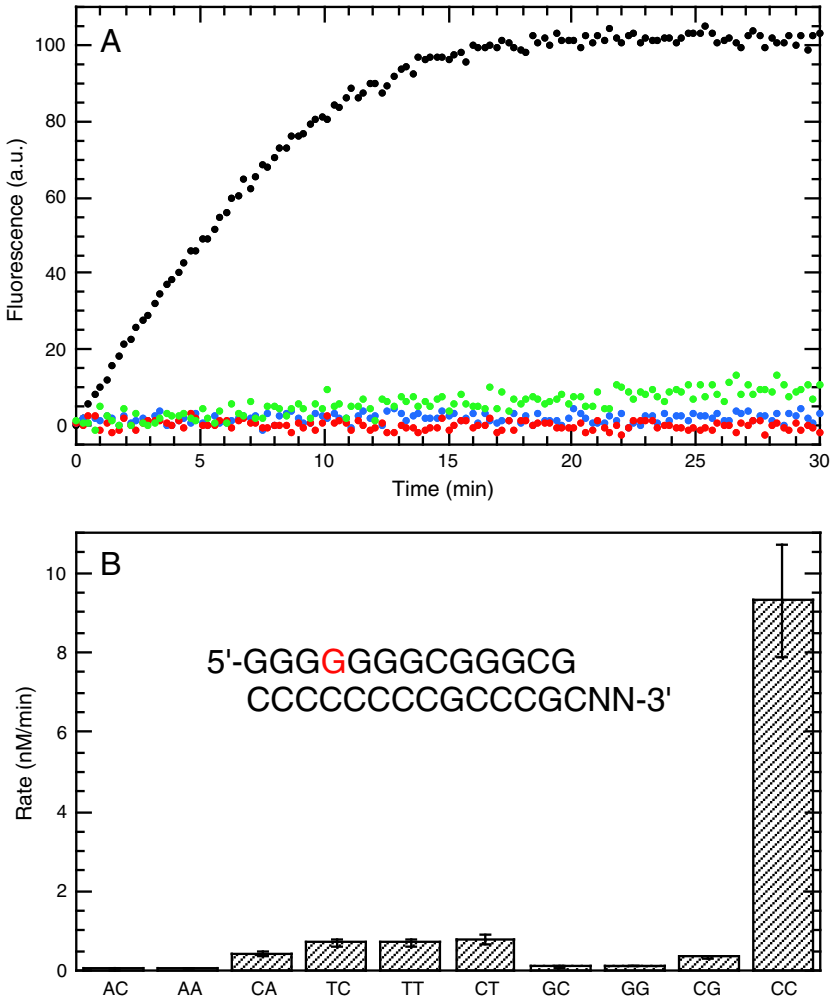

Fig. 6. Incorporation of guanines against A, G and T. (A) Time course of dGMP incorporation opposite template GC (blue), GG (red), CG (green) at the 5′-end. Black points correspond to positive control with template CC at the 5′-end. All reactions were in 50 mM KCl, 2 mM $MgCl_2$, 10 mM Tris–HCl, pH 8.7 at 20 °C. (B) Histogram showing rates of dGTP-QPA performed on templates with the NN incorrect nucleotides indicated on the X axis.

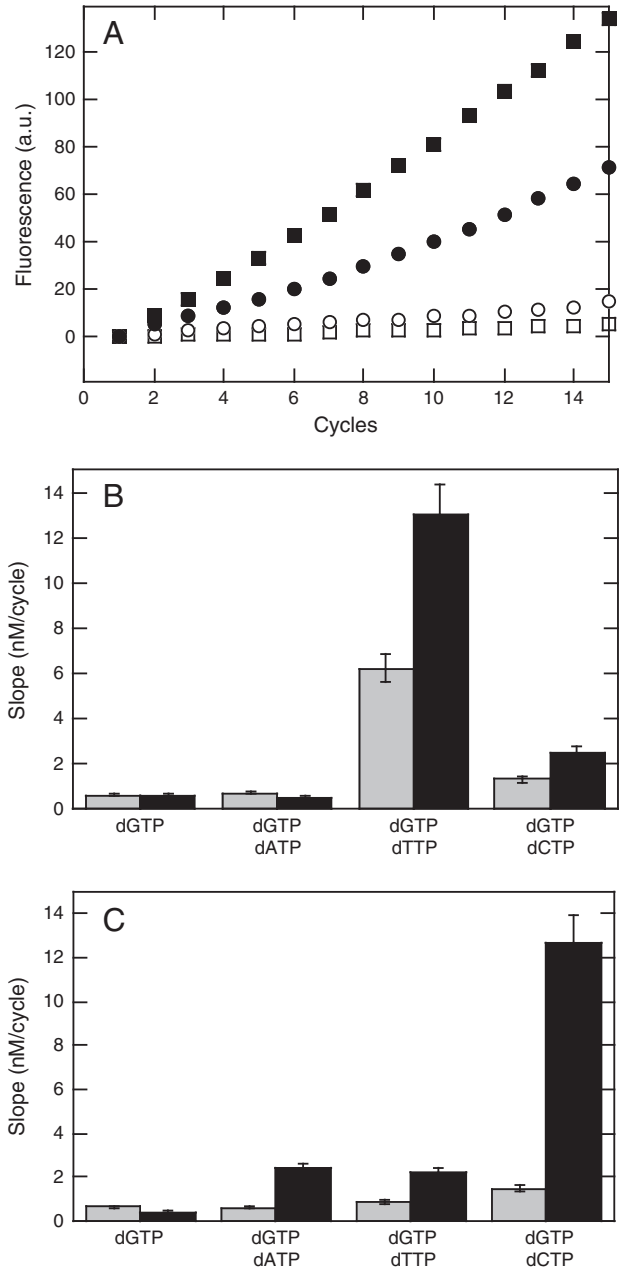

Fig. 7. Incorporation of nucleotides opposite template containing 2AP and 6MI monitored by temperature cycling QPA. (A) Templates containing 2AP (circles) and control sequence with A instead of 2AP (squares) in the presence of dGTP + dTTP (filled symbols) and dGTP (open symbols). All experiments were in 50 mM KCl, 2 mM $MgCl_2$, 10 mM Tris–HCl, pH 8.7 at 20 °C. Histograms for templates with 2AP (B) and 6MI (C) showing slopes of the temperature cycling QPA. Gray bars correspond to templates with the fluorescent nucleotides and black bars correspond to control templates (in case of 2AP control sequence has A and in case of 6MI control sequence has G).

activity. To determine if *Taq* polymerase could incorporate other nucleotides opposite 2AP and 6MI, we designed a new QFA-based assay that uses temperature cycling and different dNTP combinations. Temperature cycling is required since primers are missing four nucleotides at the 3′-end, which inhibits spontaneous dissociation of the elongated primers from the templates. The primers are designed such that only full elongation of the template sequence, which contains non-natural nucleotides at the loop position of the G3T sequence, can create a fluorescent signal. In other words, after incorporation of nucleotides at the position of interest, the polymerase should add three guanines. Initially, we performed the assay only in the presence of dGTPs. As seen from Fig. 7B and C (far left gray columns), and as expected from previous measurements, the polymerase is not able to incorporate dGTP against 2AP or 6MI. In the next experiments, we used each dNTP in combination with dGTP; the results demonstrated that only in the case of dTTP opposite template 2AP does QPA reveal significant activity. However, even in this case, the QPA rate is around two times slower than that of the control experiment with template A instead of 2AP. In all other cases, including dCTP opposite template 6MI, QPA does not reveal any measurable activity. These results are in agreement with reported data, which demonstrates good tolerance of 2AP by DNA polymerases [29] and no significant incorporation of any nucleotides opposite of 6MI [30].

4. Conclusions

The role of reaction components and experimental conditions in QPA reactions was examined in detail in this work. Studies carried out with the QPA primers missing one, two and three nucleotides at the 3′-end suggest that the driving force for isothermal QPA is the result of the thermal stability difference between primer/template and product complexes. While the primers missing one and two guanines are able to self-dissociate from the template upon polymerase elongation, isothermal QPA is not observed with the primer missing three nucleotides. The temperature dependence of QPA rates closely correlates with the melting behavior of the complexes, and QPA reaches its maximum rate at temperatures 2–3 °C higher than the melting temperature of the primer/template complexes. The reactions conducted in the presence of only dGTP showed that QPA is more efficient in the absence of other dNTPs, and good activity was observed even at unusually low concentration of dGTP. The QPA-based real-time assays also show that *Taq* polymerase is able to incorporate thymidines opposite of 2AP, which is desirable for exponential QPA. In contrast, no significant incorporation was observed opposite of 6MI. The later feature can be explored in further development of exponential QPA employing nicking enzymes (unpublished data).

Taking together, the data reported here create a framework for the further development and applications of QPA in nucleic acid-based diagnostics. Although the 15-nt primer-binding site of QPA, CCC ACCCACCCACCC, is found multiple times in the human genome, false positive signals can be avoided by elongating the QPA primer at the 3′-end. In addition, since QPA uses a universal primer, the complement must be incorporated into a target sequence. Recently, we demonstrated that this can be accomplished by two cycles of traditional PCR in which the 5′ ends of both forward and reverse primers have quadruplex sequences [3]. Therefore, QPA represents a universal approach for amplifying any target sequence of interest.

Acknowledgments

This work was supported by a grant from the Bill & Melinda Gates Foundation through the Grand Challenges in Global Health initiative; Shota Gogichaishvili acknowledges support from Shota Rustaveli National Science Foundation (Tbilisi, Georgia).

References

[1] O. Clerc, G. Greub, Routine use of point-of-care tests: usefulness and application in clinical microbiology, Clinical Microbiology and Infection 16 (2010) 1054–1061.
[2] A. Niemz, T.M. Ferguson, D.S. Boyle, Point-of-care nucleic acid testing for infectious diseases, Trends in Biotechnology 29 (2011) 240–250.
[3] B.I. Kankia, Self-dissociative primers for nucleic acid amplification and detection based on DNA quadruplexes with intrinsic fluorescence, Analytical Biochemistry 409 (2011) 59–65.
[4] B.I. Kankia, L.A. Marky, DNA, RNA, and DNA/RNA oligomer duplexes: a comparative study of their stability, heat, hydration and Mg(2+) binding properties, The Journal of Physical Chemistry. B 103 (1999) 8759–8767.
[5] L.A. Marky, K.J. Breslauer, Calculating thermodynamic data for transitions of any molecularity from equilibrium melting curves, Biopolymers 26 (1987) 1601–1620.
[6] B.I. Kankia, Optical absorption assay for strand-exchange reactions in unlabeled nucleic acids, Nucleic Acids Research 32 (2004) e154.

[7] B.I. Kankia, A real-time assay for monitoring nucleic acid cleavage by quadruplex formation, Nucleic Acids Research 34 (2006) e141.
[8] N.Q. Do, K.W. Lim, M.H. Teo, B. Heddi, A.T. Phan, Stacking of G-quadruplexes: NMR structure of a G-rich oligonucleotide with potential anti-HIV and anticancer activity, Nucleic Acids Research 39 (2011) 9448–9457.
[9] S. Kelley, S. Boroda, K. Musier-Forsyth, B.I. Kankia, HIV-integrase aptamer folds into a parallel quadruplex: a thermodynamic study, Biophysical Chemistry 155 (2011) 82–88.
[10] M. Zuker, Mfold web server for nucleic acid folding and hybridization prediction, Nucleic Acids Research 31 (2003) 3406–3415.
[11] C.M. Joyce, S.J. Benkovic, DNA polymerase fidelity: kinetics, structure, and checkpoints, Biochemistry 43 (2004) 14317–14324.
[12] R.D. Kuchta, V. Mizrahi, P.A. Benkovic, K.A. Johnson, S.J. Benkovic, Kinetic mechanism of DNA polymerase I (Klenow), Biochemistry 26 (1987) 8410–8417.
[13] S.S. Patel, I. Wong, K.A. Johnson, Pre-steady-state kinetic analysis of processive DNA replication including complete characterization of an exonuclease-deficient mutant, Biochemistry 30 (1991) 511–525.
[14] K. Datta, V.J. LiCata, Thermodynamics of the binding of *Thermus aquaticus* DNA polymerase to primed-template DNA, Nucleic Acids Research 31 (2003) 5590–5597.
[15] K. Datta, A.J. Wowor, A.J. Richard, V.J. LiCata, Temperature dependence and thermodynamics of Klenow polymerase binding to primed-template DNA, Biophysical Journal 90 (2006) 1739–1751.
[16] B.I. Kankia, L.A. Marky, Folding of the thrombin aptamer into a G-quadruplex with Sr(2+): stability, heat, and hydration, Journal of the American Chemical Society 123 (2001) 10799–10804.
[17] R.D. Gray, J.B. Chaires, Kinetics and mechanism of K+- and Na+-induced folding of models of human telomeric DNA into G-quadruplex structures, Nucleic Acids Research 36 (2008) 4191–4203.
[18] N.V. Hud, F.W. Smith, F.A. Anet, J. Feigon, The selectivity for K+ versus Na+ in DNA quadruplexes is dominated by relative free energies of hydration: a thermodynamic analysis by 1H NMR, Biochemistry 35 (1996) 15383–15390.
[19] E. Tan, B. Erwin, S. Dames, T. Ferguson, M. Buechel, B. Irvine, K. Voelkerding, A. Niemz, Specific versus nonspecific isothermal DNA amplification through thermophilic polymerase and nicking enzyme activities, Biochemistry 47 (2008) 9987–9999.
[20] E. Tan, B. Erwin, S. Dames, K. Voelkerding, A. Niemz, Isothermal DNA amplification with gold nanosphere-based visual colorimetric readout for herpes simplex virus detection, Clinical Chemistry 53 (2007) 2017–2020.
[21] M.F. Goodman, K.D. Fygenson, DNA polymerase fidelity: from genetics toward a biochemical understanding, Genetics 148 (1998) 1475–1482.
[22] T.A. Kunkel, K. Bebenek, DNA replication fidelity, Annual Review of Biochemistry 69 (2000) 497–529.
[23] R. Mitra, B.M. Pettitt, G.L. Rame, R.D. Blake, The relationship between mutation rates for the (C-G)–>(T-A) transition and features of T-G mispair structures in different neighbor environments, determined by free energy molecular mechanics, Nucleic Acids Research 21 (1993) 6028–6037.
[24] S.M. Law, R. Eritja, M.F. Goodman, K.J. Breslauer, Spectroscopic and calorimetric characterizations of DNA duplexes containing 2-aminopurine, Biochemistry 35 (1996) 12329–12337.
[25] L.W. McLaughlin, T. Leong, F. Benseler, N. Piel, A new approach to the synthesis of a protected 2-aminopurine derivative and its incorporation into oligodeoxynucleotides containing the Eco RI and Bam HI recognition sites, Nucleic Acids Research 16 (1988) 5631–5644.
[26] M.E. Hawkins, Fluorescent pteridine probes for nucleic acid analysis, Methods in Enzymology 450 (2008) 201–231.
[27] M.E. Hawkins, Synthesis, purification and sample experiment for fluorescent pteridine-containing DNA: tools for studying DNA interactive systems, Nature Protocols 2 (2007) 1013–1021.
[28] M.E. Hawkins, W. Pfleiderer, F.M. Balis, D. Porter, J.R. Knutson, Fluorescence properties of pteridine nucleoside analogs as monomers and incorporated into oligonucleotides, Analytical Biochemistry 244 (1997) 86–95.
[29] E. Fidalgo da Silva, S.S. Mandal, L.J. Reha-Krantz, Using 2-aminopurine fluorescence to measure incorporation of incorrect nucleotides by wild type and mutant bacteriophage T4 DNA polymerases, Journal of Biological Chemistry 277 (2002) 40640–40649.
[30] K. Datta, N.P. Johnson, G. Villani, A.H. Marcus, P.H. von Hippel, Characterization of the 6-methyl isoxanthopterin (6-MI) base analog dimer, a spectroscopic probe for monitoring guanine base conformations at specific sites in nucleic acids, Nucleic Acids Research 40 (2012) 1191–1202.